

SEMr2: Table Separation Line Detection Based on Conditional Convolution

Zhenrong Zhang^{*1,2}, Pengfei Hu¹, Jiefeng Ma¹, Jun Du^{†1},
Jianshu Zhang², Huihui Zhu², Baocai Yin², Bing Yin², Cong Liu²
¹ University of Science and Technology of China
² iFLYTEK AI Research

Abstract

Table structure recognition is an indispensable element for enabling machines to comprehend tables. Its primary purpose is to identify the internal structure of a table. Nevertheless, due to the complexity and diversity of their structure and style, it is highly challenging to parse the tabular data into a structured format that machines can comprehend. In this work, we adhere to the principle of the split-and-merge based methods and propose an accurate table structure recognizer, termed SEMr2 (SEM: Split, Embed and Merge). Unlike the previous works in the “split” stage, we aim to address the table separation line instance-level discrimination problem and introduce a table separation line detection strategy based on conditional convolution. Specifically, we design the “split” in a top-down manner that detects the table separation line instance first and then dynamically predicts the table separation line mask for each instance. The final table separation line shape can be accurately obtained by processing the table separation line mask in a row-wise/column-wise manner. To comprehensively evaluate the SEMr2, we also present a more challenging dataset for table structure recognition, dubbed iFLYTAB, which encompasses multiple style tables in various scenarios such as photos, scanned documents, etc. Extensive experiments on publicly available datasets (e.g. SciTSR, PubTabNet and iFLYTAB) demonstrate the efficacy of our proposed approach. The code and iFLYTAB dataset will be made publicly available upon acceptance of this paper.

1. Introduction

In this era of knowledge and information, document is a significant source of information for numerous cognitive processes such as knowledge database creation, optical character recognition (OCR), document retrieval, etc. As a particular entity, the tabular structure is very commonly en-



Figure 1. Some table samples in the iFLYTAB dataset. (a)-(b) are wired tables. (c)-(e) are wireless tables.

countered in documents. These tabular structures convey important information in a concise form. They are highly prevalent in domains such as finance, administration, research, and even archival documents. Table structure recognition (TSR) aims to recognize the table internal structure to the machine readable data mainly presented in two formats: logical structure and physical structure [33]. More precisely, logical structure only contains every cell’s row and column spanning information, while the physical one additionally contains bounding box coordinates of cells. Therefore, TSR as a precursor to contextual table understanding will be beneficial in a wide range of applications [27, 26].

Limited by the training datasets [7, 2, 37, 36] used for TSR, most previous works [28, 24, 35, 26] focus on document images that are obtained from digital documents (e.g., PDF files). In such a scenario, the table images are cropped under optimal imaging conditions and are often horizontally (or vertically) aligned with a clean background and distinct table structures. However, in some real-world applications, document images may be captured by mobile cameras. Many camera-captured document images are of poor image quality, and tables contained in them may be distorted (even curved) or contain noises, which makes TSR even more chal-

*Work done during an internship at iFLYTEK AI Research.

†Correspondence Author.

lenging. Although the WTW dataset proposed recently [17] contains table images from natural scenes, it only focuses on wired tables. Parsing wireless tables is a relatively more difficult task due to the lack of visual cues to delimit cells, columns and rows. To comprehensively evaluate the performance of TSR, we present a large-scale dataset in this paper, dubbed iFLYTAB. As shown in Figure 1, the table images in the iFLYTAB dataset are collected from various scenarios, and contain both wired and wireless tables.

Considering that a table is composed of a set of table cells and each table cell is composed of one or more basic table grids, the recently proposed split-and-merge based methods [28, 35, 20] consider table grids as the fundamental processing units. These methods recognize the table structure as the following pipeline: 1) split table into basic table grid pattern 2) merge grid elements to recover table cells that span multiple rows or columns. When the TSR is performed in this way, once the “split” stage predicts erroneous results, it is difficult for the “merge” stage to rectify them. Therefore, it is essential to make the model detect table grids more accurately. The previous methods [28, 35, 20] complete the first stage in a bottom-up manner. Specifically, they first apply semantic segmentation [16] to predict table row/column separation lines, and then represent the intersection of detected row/column separation lines as table grids. However, segmenting table row/column separation lines in a pixel-wise manner is imprecise due to the limited receptive field. In addition, it necessitates complex mask-to-line algorithms to extract the table separation lines from the predicted segmentation results.

In this work, we follow the split-and-merge based method SEM [35], and introduce an accurate table structure recognizer, termed SEMv2. Distinct from previous segmentation-based methods [35, 26, 28, 20] in the “split” stage, we aim to distinguish each table separation line and formulate table separation line detection as an instance segmentation task. Specifically, the table separation line mask generation is decoupled into a mask kernel prediction and a mask feature learning, which are responsible for generating convolution kernels and the feature maps to be convolved with respectively. Accurate table row/column separation lines can be easily obtained by processing table row/column separation line masks in a column-wise/row-wise manner. Moreover, compared to the sequence decoder in the “merge” stage in [35], we propose a parallel decoder based on conditional convolution to process the merging of basic table grids, which increases the decoding speed. To comprehensively evaluate the SEMv2, we also introduce a new large-scale TSR dataset iFLYTAB, which contains multiple style tables in several scenes like photos, scanned documents, etc.

The main contributions of this paper are as follows:

- Following the split-and-merge based methods, we propose the SEMv2, which introduces a novel instance

segmentation framework for the table separation line detection in the “split” stage, making the “split” more robust in various scenes.

- We release the iFLYTAB dataset, which is collected from various scenarios and manually annotated carefully, to the community for advancing related research.
- Based on our proposed method, we achieve state-of-the-art performance on publicly available datasets SciTSR, PubTabNet and iFLYTAB.

2. Related Work

2.1. Existing Datasets

The first dataset for addressing TSR is ICDAR-2013 [7], but its data size is limited (96 tables for training and 156 tables for testing). To meet the requirement of data-driven approaches for TSR, large-scale datasets such as TableBank [11] and PubTabNet [37] are proposed, but incomplete annotations still impede their development. Recently, FinTabNet [36] and SciTSR [2] add the cell coordinates and row-column information to become relatively comprehensive datasets for TSR. Although dataset scale has been significantly increased, these datasets solely focus on digital documents (e.g., PDF files). Recently, a new dataset WTW [17], which contains tables in multiple real scenes, is introduced. However, it only focuses on wired tables, ignoring the more challenging wireless ones. To comprehensively evaluate the TSR performance, we present a new large-scale dataset iFLYTAB. Different from WTW, tables in iFLYTAB encompass both wired and wireless tables in various scenarios.

2.2. Table Structure Recognition

Due to the rapid development of deep learning in documents, many deep learning-based TSR approaches [37, 3, 35, 25] have been presented. These methods can be roughly divided into three categories: bottom-up methods, image-to-markup based methods and split-and-merge based methods.

One group of bottom-up methods [3, 23, 32] treat words or cell contents as nodes in a graph and use graph neural networks to predict whether each sampled node pair is in the same cell, row, or column. These methods rely on an assumption that the bounding boxes of words or cell contents are available as additional inputs, which are not easy to obtain from table images directly. To eliminate this assumption, another group of methods [25, 24] proposed to detect the bounding boxes of table cells directly. After cell detection, they designed some rules to cluster cells into rows and columns. However, these methods fail to handle distorted tables and tables containing a large number of empty cells.

The image-to-markup based methods [37, 6, 21] treat table structure recognition as a task similar to image-to-markup generation and directly generate the markup tags that define the structure of the table through an attention-based structure decoder. These methods rely on a large amount of training data and are inefficient as the number of table cells increases.

The split-and-merge based methods [28, 35, 20] first split a table into the basic table grid pattern, and then merge grid elements to recover table cells. Previous methods utilize semantic segmentation [16] for identifying rows, columns within tables in the “split” stage. However, segmenting table row/column separation lines in a pixel-wise manner is inaccurate due to the limited receptive field. In our work, we formulate the table separation line detection as the instance segmentation task.

2.3. Instance Segmentation

Instance segmentation is a challenging task, as it necessitates instance-level and pixel-level predictions simultaneously. The dominant framework for instance segmentation is Mask R-CNN [8], which first detects the bounding boxes of objects and then segments the object in the box. Many works [15, 1, 10] with top performance are built on Mask R-CNN. Due to the slender shape of table separation lines, this widely utilized box-anchor based instance segmentation methods cannot be employed directly. Another approach to instance segmentation is based on dynamic filter network [4]. For example, SOLOv2 [31] and CondInst [29] learn instance-dependent convolutional kernels, which are applied to generate instance masks. Inspired by CondInst, we aim to resolve the table row/column instance-level discrimination problem, and propose the conditional table separation line detection strategy.

3. iFLYTAB

iFLYTAB collects table images of various styles from different scenarios. Specifically, as shown in Figure 2, we collect both wired and wireless tables from digital documents, and camera-captured photos. As shown in Table 1, the table images of existing datasets (e.g. SciTSR, PubTabNet, etc.) are mainly derived from digital PDF files. However, iFLYTAB includes table images captured by cameras, which contain complex image backgrounds and non-rigid image deformation. Although WTW provides table images in the photographic scenario, it ignores the more challenging wireless tables. In terms of data labeling, we provide full annotation for each table image including physical coordinates and row/column information. We randomly select approximately 70% of the table images as the training set, and the rest data samples are used for testing. Finally, our iFLYTAB dataset has 12,104 training samples and 5,187 testing ones. Please refer to the Appendix for more details

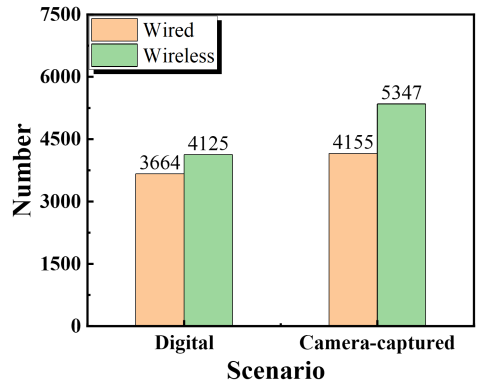


Figure 2. Statistics of the iFLYTAB datasets.

Table 1. Comparison with other existing datasets.

Dataset	Digital		Camera-captured	
	Wired	Wireless	Wired	Wireless
ICDAR-2013 [7]	✓	✓	✗	✗
SciTSR [2]	✓	✓	✗	✗
PubTabNet [37]	✓	✓	✗	✗
WTW [18]	✓	✗	✓	✗
iFLYTAB	✓	✓	✓	✓

about the proposed dataset.

4. Method

The schematic of our approach is depicted in Figure 3. SEMv2 adheres to the split-and-merge based methodology of its predecessor, SEM, and is primarily comprised of three components: the splitter, the embedder, and the merger. The splitter takes the table image as input and predicts the fine grid structure of the table. The embedder extracts the grid-level feature representation of each basic table grid. The merger predicts which grids should be merged to recover the whole table structure. Subsequently, we will elucidate each component.

4.1. Splitter

Given an input table image $I \in \mathbb{R}^{H \times W \times 3}$, as illustrated in Figure 3, the objective of the splitter is to predict the table grid structure with a set of grid bounding boxes $B \in \mathbb{R}^{M \times N \times 4}$, where M , N are the number of rows and columns occupied by the table grid structure respectively. Previous split-and-merge based methods apply the semantic segmentation to predict all table row/column separation lines in one mask and subsequently represent the intersection of detected row/column separation lines as grid bounding boxes B . In contrast to prior methods, we formulate table separation line detection as an instance segmentation task and endeavor to predict an individual mask for each table

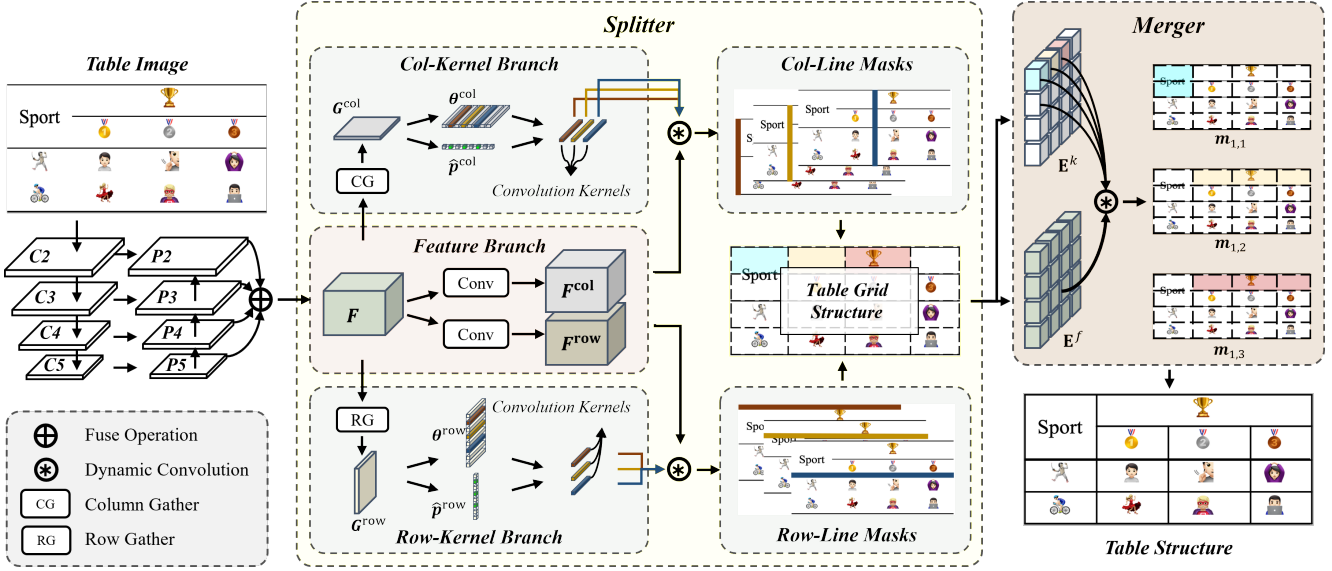


Figure 3. The overall architecture of SEMv2. F is the feature map generated by fusing the FPN feature maps (P_2 to P_5). The *Splitter* module consists of *Kernel Branch* and *Feature Branch*, and predicts table separation lines between different columns or rows, which can be further processed to obtain the *Table Grid Structure*. The *Merger* module predicts the table cell to which each table grid belongs. We omit the *Embedder* module for simplicity.

row/column separation line.

The overall architecture of our splitter is depicted in Figure 3. The ResNet-34 [9] with FPN [13] is utilized to generate a feature pyramid with four feature maps $\{P_2, P_3, P_4, P_5\}$, whose scales are $1/4, 1/8, 1/16, 1/32$ respectively. To amalgamate the information from all levels of the FPN pyramid into a single output F , we also propose a straightforward fuse operation as follows:

$$F = P_2 + \text{Up}_{1\times}(P_3) + \text{Up}_{2\times}(P_4) + \text{Up}_{3\times}(P_5) \quad (1)$$

where $\text{Up}_{n\times}$ denotes the n times bilinear upsample operation. $F \in \mathbb{R}^{\frac{H}{4} \times \frac{W}{4} \times C}$, where C denotes the number of feature channels.

Inspired by CondInst [29], we decouple the table separation line mask generation into a feature branch and a kernel branch. The feature branch contains two 1×1 convolution layers for generating $F^{\text{col}}/F^{\text{row}}$, which will be convoluted with convolution kernels from kernel branches to predict separation line masks. Since the table separation lines are usually slender and traverse the entire table image, it is necessary to design a kernel branch that has a broader receptive field. To address this issue, we propose the Gather module to capture the horizontal/vertical visual clues as shown in Figure 4.

Taking the Column Gather as an example, we first conduct three repeated down-sampling operations on F , and each operation is composed of a sequence of a 2×1 max-pooling layer, a 3×3 convolutional layer and a ReLU activation function. The down-sampled feature map $\tilde{F}^{\text{col}} \in \mathbb{R}^{\frac{H}{32} \times \frac{W}{4} \times C}$

will be taken as the input of two following spatial CNN modules [22]. The first spatial CNN module divides the feature map into $H/32$ slices, which are denoted as $\mathcal{S}^{\text{td}} = \{s_i^{\text{td}} \in \mathbb{R}^{1 \times \frac{W}{4} \times C} \mid i = 1, 2, \dots, \frac{H}{32}\}$. Specifically, the topmost slice s_1^{td} is convolved by a 1×5 convolution layer, and its output feature map is merged with the next slice s_2^{td} by element-wise addition. This procedure is done iteratively so that the information can be propagated from the topmost to the bottommost effectively. The second spatial CNN module transmits information in a reversed direction. In this way, each pixel in the output feature map can leverage the structural information from both sides to enhance its feature representation ability. $G^{\text{col}} \in \mathbb{R}^{1 \times \frac{W}{4} \times C}$ is obtained by taking the row mean of the enhanced feature map. We add a linear transformation following the G^{col} to predict C -dimensional output $\theta^{\text{col}} \in \mathbb{R}^{1 \times \frac{W}{4} \times C}$. θ^{col} will be used as the weights of a 1×1 convolution layer to predict table column separation line masks. We also detect table column separation line instance by predicting $\hat{p}^{\text{col}} \in \mathbb{R}^{1 \times \frac{W}{4} \times 1}$ through a linear transformation. The loss function on \hat{p}^{col} is formulated as follows:

$$\mathcal{L}_{\text{inst}}^{\text{col}} = \sum_{i=1}^{W/4} \frac{L_{\text{bce}}(\hat{p}_i^{\text{col}}, \tilde{p}_i^{\text{col}})}{W/4} \quad (2)$$

where L_{bce} is the binary cross-entropy loss, \tilde{p}^{col} denotes the ground-truth distribution of starting points of table column separation lines on the x -axis. \tilde{p}_i^{col} is 1 if the start point of a table column separation line is located in the i -th column, otherwise 0. To eliminate the duplicated predic-

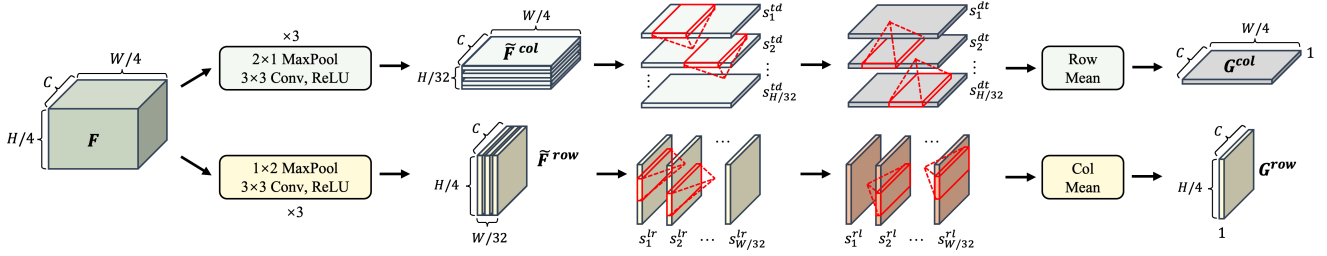


Figure 4. Illustration of the Gather architecture. The upper part is the Column Gather. The lower part is the Row Gather.

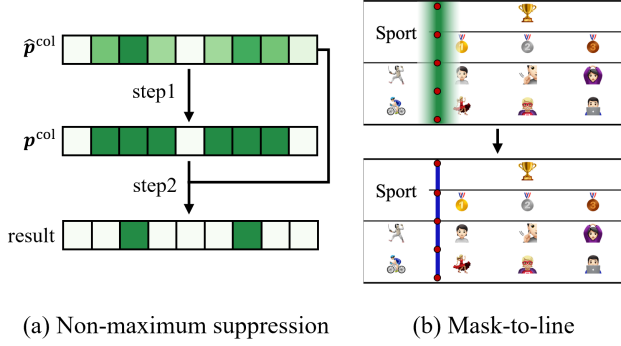


Figure 5. The illustration of Post-processing.

tions of the starting point of a table column separation line in \hat{p}^{col} , as shown in Figure 5(a), we perform non-maximum suppression as follows: 1) binarize the \hat{p}^{col} into p^{col} , 2) for the continuous pixels whose value equals 1 in p^{col} , the pixel with maximum score in \hat{p}^{col} will be selected to represent a table column separation line instance.

According to the detected table separation line instance, we select convolution kernels from θ^{col} to conduct dynamic convolution with F^{col} to predict table column separation line masks $\hat{F}^{\text{col}} \in \mathbb{R}^{\frac{H}{4} \times \frac{W}{4} \times N^{\text{col}}}$, where N^{col} represents the number of detected table column separation line instances. The loss function on \hat{F}^{col} is defined as follow:

$$\mathcal{L}_s^{\text{col}} = \frac{1}{N^{\text{col}}} \sum_{k=1}^{N^{\text{col}}} \sum_{i=1}^H \sum_{j=1}^W \frac{L_{fl}(\hat{F}_{i,j,k}^{\text{col}}, \tilde{F}_{i,j,k}^{\text{col}})}{\sum_{i=1}^H \sum_{j=1}^W \tilde{F}_{i,j,k}^{\text{col}}} \quad (3)$$

in which

$$L_{fl}(x, y) = \begin{cases} \alpha (1 - \sigma(x))^\gamma \log\left(\frac{1}{\sigma(x)}\right), & \text{if } y = 1 \\ (1 - \alpha) \sigma(x)^\gamma \log\left(\frac{1}{1 - \sigma(x)}\right), & \text{if } y = 0 \end{cases} \quad (4)$$

where \tilde{F}^{col} denotes the ground-truth of table column separation line masks. $\tilde{F}_{i,j,k}^{\text{col}}$ is 1 if the pixel in i^{th} row, j^{th} column and k^{th} channel belongs to k^{th} table column line, otherwise 0. The function L_{fl} is actually the sigmoid focal loss [12] and the σ is the sigmoid function.

Considering the table column separation lines are typically spread through vertical direction, we process \hat{F}^{col} in a

row-wise manner to obtain the final table column separation line. Specifically, as shown in Figure 5(b), given a table column separation line mask, we first find the maximum score of each row, which is presented as a set of red dots as shown in Figure 5(b). The table column separation line can be obtained by connecting these red dots together. The grid bounding boxes \mathbf{B} can be derived from the intersection of table row/column separation lines.

4.2. Embedder

The embedder aims to extract the grid-level feature representations $\mathbf{E} \in \mathbb{R}^{M \times N \times D}$, where D is the number of feature channels. We take the image-level feature map \mathbf{F} and the well-divided table grids \mathbf{B} obtained from the splitter as input, and apply the RoIAlign [8] to extract a fixed size $R \times R$ feature map $\hat{e}_{i,j} \in \mathbb{R}^{R \times R \times C}$ for each grid.

$$\hat{e}_{i,j} = \text{RoIAlign}_{R \times R}(\mathbf{F}, \mathbf{b}_{i,j}) \quad (5)$$

Then two linear transformations with a ReLU function are conducted on $\hat{e}_{i,j}$ to obtain the D -dimension output:

$$e_{i,j} = \max(0, \hat{e}_{i,j} \mathbf{W}_1 + \mathbf{b}_1) \mathbf{W}_2 + \mathbf{b}_2 \quad (6)$$

where \mathbf{W}_1 and \mathbf{W}_2 are learned projection matrices, \mathbf{b}_1 and \mathbf{b}_2 are learned biases. So far, the features of each basic table grid are still independent of each other. Therefore, we introduce the transformer [30] to capture long-range dependencies on table grid elements and utilize its output as the final grid-level features \mathbf{E} .

4.3. Merger

The merger takes the grid-level features \mathbf{E} as input and yields a set of merged maps $\mathbf{M} = \{\mathbf{m}_{1,1}, \dots, \mathbf{m}_{M,N}\}$, $\mathbf{m}_{i,j} \in \{0,1\}^{M \times N}$, $i \in \{1, \dots, M\}$, $j \in \{1, \dots, N\}$. Following the approach of the splitter, as illustrated in Figure 3, we use a feature branch and a kernel branch to predict \mathbf{M} jointly. Each branch contains only one 1×1 convolution layer to generate feature maps $\mathbf{E}^f \in \mathbb{R}^{M \times N \times D}$ and kernel parameters $\mathbf{E}^k \in \mathbb{R}^{M \times N \times D}$. We first convolute the feature map \mathbf{E}^f with kernel parameter $e_{i,j}^k$, which is utilized as the weights of a 1×1 convolution layer, to predict the merged map

Table 2. Comparisons of different designed systems from T1 to T6 on different datasets. ‘‘InstSeg’’ means the Instance Segmentation method which is the proposed splitter in this paper. ‘‘SemaSeg’’ means the Semantics Segmentation method which follows the splitter in SEM [35]. ‘‘ParaDec’’ means the Parallel Decoder which is the proposed merger in this paper. ‘‘SeqDec’’ means the Sequence Decoder which follows the merger in SEM [35].

System	Splitter		Gather	Merger		SciTSR				iFLYTAB			
	InstSeg	SemaSeg		ParaDec	SeqDec	P	R	F1	FPS	P	R	F1	TEDS-Struct
T1	✓	✗	✓	✓	✗	99.3	99.2	99.3	7.3	93.8	93.3	93.5	92.0
T2	✗	✓	✓	✓	✗	99.1	98.5	98.8	-	81.9	72.7	77.0	75.8
T3	✓	✗	✗	✓	✗	-	-	-	-	91.1	89.8	90.4	89.3
T4	✓	✗	✓	✗	✗	99.1	97.4	98.2	8.9	-	-	-	-
T5	✓	✗	✓	✗	✓	99.3	99.2	99.2	2.9	-	-	-	-

$\hat{m}_{i,j} \in [0, 1]^{M \times N}$. The loss function is formulated as follows:

$$\mathcal{L}_m = \frac{1}{M \times N} \sum_{i=1}^M \sum_{j=1}^N \frac{L_{fl}(\hat{m}_{i,j}, \tilde{m}_{i,j})}{\|\tilde{m}_{i,j}\|_1} \quad (7)$$

where $\|\cdot\|_1$ is the L1 norm, the function L_{fl} has been defined in Eq. 4, $\tilde{m}_{i,j} \in \{0, 1\}^{M \times N}$ denotes the merged map ground-truth of the i^{th} row, j^{th} column table grid. If the value of $\tilde{m}_{i,j}$ is equal to 1, then it indicates that the corresponding grid is associated with the identical table cell; otherwise, 0. The final merged map $m_{i,j}$ can be obtained by binarizing $\hat{m}_{i,j}$.

5. Experiment

In this section, we perform extensive experiments on the SciTSR, PubTabNet and the proposed iFLYTAB dataset to verify the effectiveness of SEMv2. We first introduce the relevant datasets and metrics, and then demonstrate the implementation details of our method. We also conduct ablation studies to analyze the effectiveness of our proposed splitter, gather and merger. Our model is compared with state-of-the-art methods on public benchmark datasets.

5.1. Datasets

SciTSR comprises of 12,000 training samples and 3,000 testing samples of axis-aligned tables extracted from the scientific literature. Furthermore, it also selects all the 716 complex tables from the test set as a more challenging test subset, called SciTSR-COMP.

PubTabNet contains 500,777 training samples and 9,115 validating samples. All tables are also axis-aligned and collected from scientific articles.

iFLYTAB contains 12,103 training samples and 5,188 testing samples. In addition to the axis-aligned digital documents, the collected table images also include images taken by cameras, which are more challenging due to the complicated background and non-rigid image deformation.

5.2. Metric

The F1-Measure and the Tree-Edit-Distance-based Similarity (TEDS) metric are used to evaluate the performance of our model. The F1-Measure measures the percentage of correctly detected pairs of adjacent cells, where both cells are detected correctly and identified as neighbors. TEDS [37] measures the similarity of the tree structure of tables. Since taking OCR errors into account may lead to an unfair comparison due to the different OCR models used by various TSR methods. We employ a modified version of TEDS, called TEDS-Struct, which only evaluates table structure recognition accuracy while disregarding OCR results.

5.3. Implementation Details

The ResNet-34 as our backbone is pre-trained on ImageNet [5]. The number of feature channels C and D is set to 256 and 512 respectively. The pool size $R \times R$ of RoIAlign in the embedder is set to 3×3 . The hyperparameters α and γ of sigmoid focal loss L_{fl} are set to 0.25 and 2. The threshold for binarization operations is set to 0.5.

The training objective of our model is to minimize the table row/column separation line segmentation loss ($\mathcal{L}_s^{row}/\mathcal{L}_s^{col}$), the table row/column separation line instance classification loss ($\mathcal{L}_{inst}^{row}/\mathcal{L}_{inst}^{col}$), and the cell merge loss (\mathcal{L}_m). The objective function for optimization is shown as follows:

$$O = \lambda_1 \mathcal{L}_s^{row} + \lambda_1 \mathcal{L}_s^{col} + \lambda_2 \mathcal{L}_{inst}^{row} + \lambda_2 \mathcal{L}_{inst}^{col} + \lambda_3 \mathcal{L}_m \quad (8)$$

In our experiments, we set $\lambda_1 = \lambda_2 = \lambda_3 = 1$. We employ the ADADELTA [34] for optimization, with the following hyperparameters: $\beta_1 = 0.9$, $\beta_2 = 0.999$ and $\varepsilon = 10^{-9}$. We set the learning rate using the cosine annealing schedule [19] with the following hyper parameters: $\eta_{min} = 10^{-6}$ and $\eta_{max} = 10^{-4}$. We use the Nvidia Telsa V100 GPU with 32GB RAM memory for our experiments. The whole framework is implemented using PyTorch.

5.4. Ablation Study

In order to investigate the effect of each component, we conduct ablation experiments through several designed sys-



Figure 6. The segmentation results from the splitters of the designed systems T1 and T2. (a) and (b) correspond to images extracted from digital documents and camera-captured documents, respectively.

Table 3. Comparison with state-of-the-art methods. **Bold** indicates the SOTA and underline indicates the second best.

Method	SciTSR			SciTSR-COMP			PubTabNet		iFLYTAB			
	P	R	F1	P	R	F1	TEDS	TEDS-Struct	P	R	F1	TEDS-Struct
EDD [37]	-	-	-	-	-	-	88.3	-	-	-	-	-
TabStructNet [25]	92.7	91.3	92.0	90.9	88.2	89.5	-	90.1	-	-	-	-
GraphTSR [2]	95.9	94.8	95.3	96.4	94.5	95.5	-	-	-	-	-	-
SEM [35]	97.7	96.5	97.1	96.8	94.7	95.7	93.7	-	81.7	74.5	78.0	75.9
LGPMA [24]	98.2	99.3	98.8	97.3	98.7	98.0	94.6	96.7	-	-	-	-
RobusTabNet [20]	99.4	99.1	<u>99.3</u>	99.0	98.4	<u>98.7</u>	-	<u>97.0</u>	-	-	-	-
TSRFormer [14]	99.5	99.4	99.4	99.1	98.7	98.9	-	97.5	-	-	-	-
SEMv2	99.3	99.2	<u>99.3</u>	98.7	98.6	<u>98.7</u>	-	97.5	93.8	93.3	93.5	92.0

tems as shown in Table 2. The model is not modified except for the component being tested.

The effectiveness of the splitter. In contrast to the majority of previous “split-and-merge” based methods, we formulate table separation line detection in the “split” stage as an instance segmentation task rather than a semantic segmentation. To evaluate the efficacy of our proposed splitter, we devised the systems T1 and T2 as shown in Table 2. Specifically, T1 represents our proposed SEMv2, whereas T2 replaces the splitter with the one used in the previous state-of-the-art method, SEM[35]. Although the performance of T1 is only marginally better than T2 on datasets comprising axis-aligned scanned PDF documents (e.g., SciTSR), T1 exhibits a significantly superior performance on the iFLYTAB dataset. This is because the iFLYTAB dataset features camera-captured images with severe deformation, bending, or occlusions. Additionally, we present the segmentation results from splitters of both T1 and T2 in Figure 6. It can be seen that both T1 and T2 can get high-quality masks on the digital document, but on the camera-captured document, the prediction result of T2 is relatively lower. It’s very hard for the mask-to-line post-processing module to handle such low-quality masks well. In contrast, our instance segmentation based method can easily obtain the shape of the table separation line in a row-wise or column-wise manner, which is more robust to such challenging tables.

The effectiveness of the Gather. To illustrate the effectiveness of the Gather module, as shown in Ta-

ble 2, we designed a system T3, which eliminates Row-Gather/ColGather, and obtains G^{row}/G^{col} by calculating the column/row mean value of F . T1 outperforms T3 by a large margin, which demonstrates the effectiveness of the Gather module for capturing horizontal/vertical visual clues.

The efficiency of the merger. As shown in Table 2, we design the systems T1, T4 and T5 that employ different mergers. T4 eliminates the merger, while T5 substitutes it with the one utilized in SEM[35]. Though T4 exhibits slightly higher Frames Per Second (FPS) than T1, its performance deteriorates significantly as it disregards table cells that span multiple rows or columns. The comparison between T1 and T4 also illustrates the indispensability of the merger. The merger in SEM predicts the merging of grids in a step-by-step manner. As the number of table cells increases, the decoding stages of T5 rise, causing the FPS of T5 to be much lower than T1 and T4.

5.5. Comparison with State-of-the-art Methods

We compare our method with other state-of-the-art methods on three TSR datasets, including SciTSR, PubTabNet and iFLYTAB. The results are shown in Table 3. Furthermore, we visualize the prediction results of our method as shown in Figure 7.

SciTSR and PubTabNet As shown in Table 3, our method achieves competitive performance compared to state-of-the-art methods. It is worth noting that the LGPMA emerged as the winner of the ICDAR 2021 Competition on

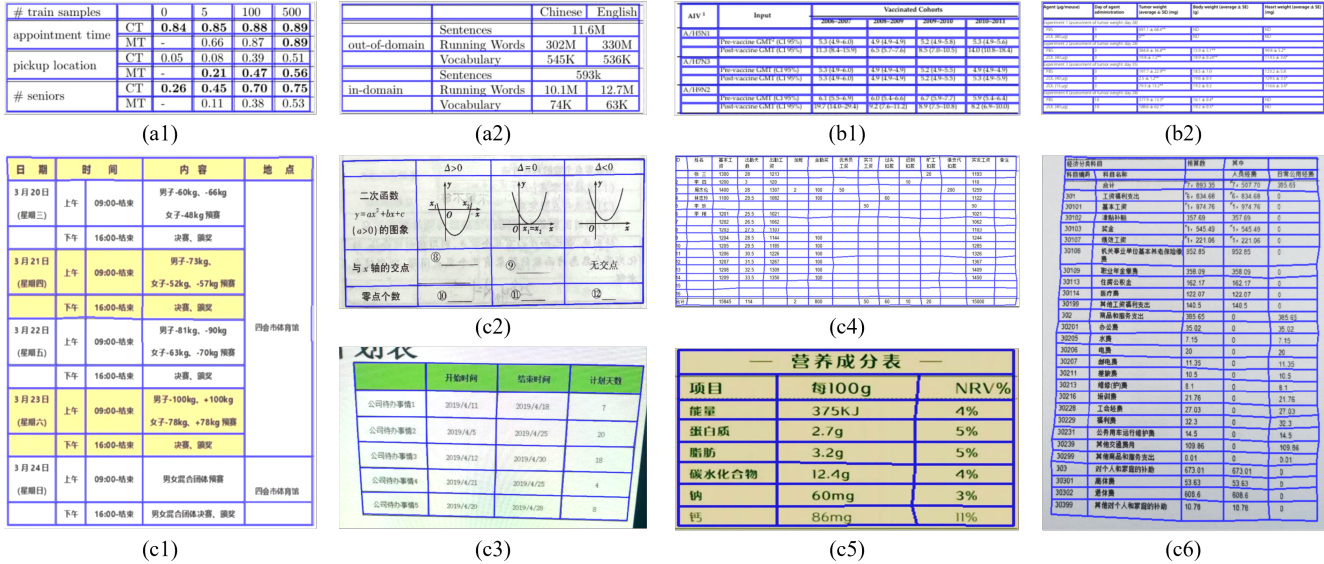


Figure 7. Some structure recognition results of SEMv2. a* refer to SciTSR, b* refer to PubTabNet, c* refer to iFLYTAB. c(1) refers to the digital wired table, c(2)~c(3) refer to camera-captured wired tables, c(4) refers to the digital wireless table, c(5)~c(6) refer to camera-captured wireless tables.

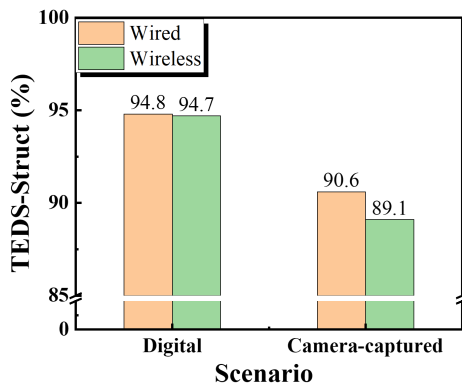


Figure 8. The Performance of SEMv2 on a series of iFLYTAB subsets.

Scientific Literature Parsing, Task B.

iFLYTAB The iFLYTAB dataset is distinct from SciTSR and PubTabNet in that it comprises table images with intricate backgrounds and non-rigid deformations. It is worth noting that detection-based methods (e.g. TabStructNet, LGPMA) are subject to the constraints that tables are free of visual rotation or perspective transformation. This condition is difficult to satisfy when table images are camera-captured. Therefore, as shown in Table 3, we re-implement the closest method, SEM [35], for a fair comparison on the iFLYTAB dataset. It can be seen that SEMv2 outperforms SEM by a large margin. As depicted in Figure 8, we also evaluate the performance of SEMv2 on different subsets of the iFLYTAB dataset. Notably, the model’s performance is comparatively lower in the camera-captured scenarios due to the subopti-

mal image qualities. Furthermore, the model’s performance is less satisfactory on wireless tables than on wired ones, as the former lack crucial visual information.

6. Conclusion

In this paper, we propose a novel method for tackling the problem of table structure recognition, SEMv2. It mainly contains three components including splitter, embedder and merger. Distinct from previous methods in the “split” stage, SEMv2 aims to distinguish each table line and formulate the table line detection as an instance segmentation task. Moreover, we propose a parallel decoder based on conditional convolution for the merger, which significantly boosting the model’s efficiency. To comprehensively evaluate the SEMv2, we also present a more challenging dataset for table structure recognition, named iFLYTAB. We collect and annotate 17291 tables (both wired and wireless type tables) in various scenarios such as camera-captured photos, scanned documents, etc. Some table images in iFLYTAB have intricate backgrounds and non-rigid deformations. The comprehensive experiments on the publicly available datasets and the iFLYTAB dataset illustrate that SEMv2 achieves a new state-of-the-art for table structure recognition. We hope our proposed iFLYTAB dataset can further advance future research on table structure recognition.

References

[1] Kai Chen, Jiangmiao Pang, Jiaqi Wang, Yu Xiong, Xiaoxiao Li, Shuyang Sun, Wansen Feng, Ziwei Liu, Jianping Shi,

- Wanli Ouyang, Chen Change Loy, and Dahua Lin. Hybrid task cascade for instance segmentation. In *CVPR*, 2019. 3
- [2] Zewen Chi, Heyan Huang, Heng-Da Xu, Houjin Yu, Wanxuan Yin, and Xian-Ling Mao. Complicated table structure recognition. *arXiv*, 2019. 1, 2, 3, 7
- [3] Zewen Chi, Heyan Huang, Heng-Da Xu, Houjin Yu, Wanxuan Yin, and Xian-Ling Mao. Complicated table structure recognition. *arXiv*, 2019. 2
- [4] Bert De Brabandere, Xu Jia, Tinne Tuytelaars, and Luc Van Gool. Dynamic filter networks. In *NIPS*, 2016. 3
- [5] Jia Deng, Wei Dong, Richard Socher, Li-Jia Li, Kai Li, and Li Fei-Fei. Imagenet: A large-scale hierarchical image database. In *CVPR*, 2009. 6
- [6] Yuntian Deng, David Rosenberg, and Gideon Mann. Challenges in end-to-end neural scientific table recognition. In *ICDAR*, 2019. 3
- [7] Max Göbel, Tamir Hassan, Ermelinda Oro, and Giorgio Orsi. Icdar 2013 table competition. In *ICDAR*, 2013. 1, 2, 3
- [8] Kaiming He, Georgia Gkioxari, Piotr Dollar, and Ross Girshick. Mask r-cnn. In *ICCV*, 2017. 3, 5
- [9] Kaiming He, Xiangyu Zhang, Shaoqing Ren, and Jian Sun. Deep residual learning for image recognition. In *CVPR*, 2016. 4
- [10] Zhaojin Huang, Lichao Huang, Yongchao Gong, Chang Huang, and Xinggang Wang. Mask scoring r-cnn. In *CVPR*, 2019. 3
- [11] Minghao Li, Lei Cui, Shaohan Huang, Furu Wei, Ming Zhou, and Zhoujun Li. Tablebank: Table benchmark for image-based table detection and recognition. In *LREC*, 2020. 2
- [12] Tsung-Yi Lin, Priya Goyal, Ross B. Girshick, Kaiming He, and Piotr Dollár. Focal loss for dense object detection. In *ICCV*, 2017. 5
- [13] Tsung-Yi Lin, Piotr Dollár, Ross Girshick, Kaiming He, Bharath Hariharan, and Serge Belongie. Feature pyramid networks for object detection. In *CVPR*, 2017. 4
- [14] Weihong Lin, Zheng Sun, Chixiang Ma, Mingze Li, Jiawei Wang, Lei Sun, and Qiang Huo. Tsrformer: Table structure recognition with transformers. In *ACM MM*, 2022. 7
- [15] Shu Liu, Lu Qi, Haifang Qin, Jianping Shi, and Jiaya Jia. Path aggregation network for instance segmentation. In *CVPR*, 2018. 3
- [16] Jonathan Long, Evan Shelhamer, and Trevor Darrell. Fully convolutional networks for semantic segmentation. In *CVPR*, 2015. 2, 3
- [17] Rujiao Long, Wen Wang, Nan Xue, Feiyu Gao, Zhibo Yang, Yongpan Wang, and Gui-Song Xia. Parsing table structures in the wild. In *ICCV*, 2021. 2
- [18] Rujiao Long, Wen Wang, Nan Xue, Feiyu Gao, Zhibo Yang, Yongpan Wang, and Gui-Song Xia. Parsing table structures in the wild. In *ICCV*, 2021. 3
- [19] Ilya Loshchilov and Frank Hutter. Sgdr: Stochastic gradient descent with warm restarts, 2017. 6
- [20] Chixiang Ma, Weihong Lin, Lei Sun, and Qiang Huo. Robust table detection and structure recognition from heterogeneous document images. *Pattern Recognition*, 2023. 2, 3, 7
- [21] Ahmed Nassar, Nikolaos Livathinos, Maksym Lysak, and Peter Staar. Tableformer: Table structure understanding with transformers. In *CVPR*, 2022. 3
- [22] Xingang Pan, Jianping Shi, Ping Luo, Xiaogang Wang, and Xiaoou Tang. Spatial as deep: Spatial cnn for traffic scene understanding. In *AAAI*, 2018. 4
- [23] Shah Rukh Qasim, Hassan Mahmood, and Faisal Shafait. Rethinking table recognition using graph neural networks. In *ICDAR*, 2019. 2
- [24] Liang Qiao, Zaisheng Li, Zhazhan Cheng, Peng Zhang, Shiliang Pu, Yi Niu, Wenqi Ren, Wenming Tan, and Fei Wu. Lgpma: Complicated table structure recognition with local and global pyramid mask alignment. In *ICDAR*, 2021. 1, 2, 7
- [25] Sachin Raja, Ajoy Mondal, and C. V. Jawahar. Table structure recognition using top-down and bottom-up cues. In *ECCV*, 2020. 2, 7
- [26] Sebastian Schreiber, Stefan Agne, Ivo Wolf, Andreas Dengel, and Sheraz Ahmed. Deepdesrt: Deep learning for detection and structure recognition of tables in document images. In *ICDAR*, 2017. 1, 2
- [27] Shoaib Ahmed Siddiqui, Muhammad Imran Malik, Stefan Agne, Andreas Dengel, and Sheraz Ahmed. Decnt: deep deformable cnn for table detection. *IEEE Access*, 2018. 1
- [28] Chris Tensmeyer, Vlad I. Morariu, Brian Price, Scott Cohen, and Tony Martinez. Deep splitting and merging for table structure decomposition. In *ICDAR*, 2019. 1, 2, 3
- [29] Zhi Tian, Chunhua Shen, and Hao Chen. Conditional convolutions for instance segmentation. In *ECCV*, 2020. 3, 4
- [30] Ashish Vaswani, Noam Shazeer, Niki Parmar, Jakob Uszkoreit, Llion Jones, Aidan N. Gomez, Lukasz Kaiser, and Illia Polosukhin. Attention is all you need. In *NIPS*, 2017. 5
- [31] Xinlong Wang, Rufeng Zhang, Tao Kong, Lei Li, and Chunhua Shen. Solov2: Dynamic and fast instance segmentation. *NIPS*, 2020. 3
- [32] Wenyuan Xue, Qingyong Li, and Dacheng Tao. Res2tim: Reconstruct syntactic structures from table images. In *ICDAR*, 2019. 2
- [33] Richard Zanibbi, Dorothea Blostein, and R. Cordy. A survey of table recognition: models, observations, transformations, and inferences. *IJDA*, 2004. 1
- [34] Matthew D. Zeiler. Adadelat: An adaptive learning rate method, 2012. 6
- [35] Zhenrong Zhang, Jianshu Zhang, Jun Du, and Fengren Wang. Split, embed and merge: An accurate table structure recognizer. *Pattern Recognition*, 2022. 1, 2, 3, 6, 7, 8
- [36] Xinyi Zheng, Douglas Burdick, Lucian Popa, Xu Zhong, and Nancy Xin Ru Wang. Global table extractor (gte): A framework for joint table identification and cell structure recognition using visual context. In *WACV*, 2021. 1, 2
- [37] Xu Zhong, Elaheh ShafieiBavani, and Antonio Jimeno Yepes. Image-based table recognition: Data, model, and evaluation. In *ECCV*, 2020. 1, 2, 3, 6, 7